TECHNICAL REPORT ARLCD-TR-81026

THE EFFECTS OF GASEOUS ATMOSPHERES ON THE PERFORMANCE CHARACTERISTICS OF ALUMINUM-SODIUM NITRATE FLARES

PATRICIA L. FARNELL
FRANCIS R. TAYLOR
ANTHONY J. BEARDELL

AUGUST 1981

US ARMY ARMAMENT RESEARCH AND DEVELOPMENT COMMAND
LARGE CALIBER
WEAPON SYSTEMS LABORATORY
DOVER, NEW JERSEY

APPROVED FOR PUBLIC RELEASE; DISTRIBUTION UNLIMITED.

REPORT DOCUMENTATION PAGE	READ INSTRUCTIONS BEFORE COMPLETING FORM

1. REPORT NUMBER Technical Report ARLCD-TR-81026	2. GOVT ACCESSION NO.	3. RECIPIENT'S CATALOG NUMBER

4. TITLE *(and Subtitle)* THE EFFECTS OF GASEOUS ATMOSPHERES ON THE PERFORMANCE CHARACTERISTICS OF ALUMINUM-SODIUM NITRATE FLARES	5. TYPE OF REPORT & PERIOD COVERED
	6. PERFORMING ORG. REPORT NUMBER

7. AUTHOR(s) Patricia L. Farnell, Francis R. Taylor, and Anthony J. Beardell	8. CONTRACT OR GRANT NUMBER(s)

9. PERFORMING ORGANIZATION NAME AND ADDRESS ARRADCOM, LCWSL Energetic Materials Division (DRDAR-LCE) Dover, NJ 07801	10. PROGRAM ELEMENT, PROJECT, TASK AREA & WORK UNIT NUMBERS

11. CONTROLLING OFFICE NAME AND ADDRESS ARRADCOM, TSD STINFO Div (DRDAR-TSS) Dover, NJ 07801	12. REPORT DATE August 1981
	13. NUMBER OF PAGES 31

14. MONITORING AGENCY NAME & ADDRESS(If different from Controlling Office)	15. SECURITY CLASS. (of this report) UNCLASSIFIED
	15a. DECLASSIFICATION/DOWNGRADING SCHEDULE

16. DISTRIBUTION STATEMENT (of this Report)

Approved for public release; distribution unlimited.

17. DISTRIBUTION STATEMENT (of the abstract entered in Block 20, if different from Report)

18. SUPPLEMENTARY NOTES

19. KEY WORDS (Continue on reverse side if necessary and identify by block number)

Aluminum-sodium nitrate flares
Pyrotechnic compositions
Atmospheric compositions

Burning rates
Luminous output
Luminous efficiency

20. ABSTRACT (Continue on reverse side if necessary and identify by block number)

The burning rates and the light outputs produced by burning binary mixtures of aluminum and sodium nitrate have been studied as a function of composition and of atmospheric content. Also studied were the effects of loading pressure upon the combustion process. The gaseous atmospheres investigated were mixtures of oxygen and nitrogen, argon, or helium. For all systems except those in which the composition was pressed at high loading pressure, the burning rate was unaffected as oxygen concentration was changed, indicating that heat and radiation feedback from the flame have only a minor

DD _{1 JAN 73} FORM 1473   EDITION OF 1 NOV 65 IS OBSOLETE

20. ABSTRACT (cont)

influence on the burning rate. Consequently, it is hypothesized that the burning rate is essentially controlled by the exothermic processes occurring at or very near to the burning surface.

For all systems, the burning composition produced low light output when oxygen was excluded from the atmosphere. With increasing oxygen content, the light output increased by a large factor. This indicates that at low oxygen concentrations much of the metal escaped from the flame unburned.

For compositions with low metal content, propagation is very difficult. It is believed that the decomposition of excess sodium nitrate removes heat from the burning surface. This heat loss reduces the rate of vaporization of the metal, causing this vaporization to become the rate controlling step. At the point at which the vaporization rate becomes considerably lower than the rate of oxidation of the metal, the flame will be quenched due to lack of fuel.

SUMMARY

The burning rates and the light outputs produced by burning binary mixtures of aluminum and sodium nitrate have been studied as a function of composition and of atmospheric content. Also studied were the effects of loading pressure upon the combustion process. The gaseous atmospheres investigated were mixtures of oxygen and nitrogen, argon, or helium. For all systems, except those in which the composition was pressed at high loading pressure, the burning rate was unaffected as oxygen concentration was changed, indicating that heat and radiation feedback from the flame have only a minor influence on the burning rate. Consequently, it is hypothesized that the burning rate is essentially controlled by the exothermic processes occurring at or very near the burning surface.

For all systems, the burning composition produced low light output when oxygen was excluded from the atmosphere. With increasing oxygen content, the light output increased by a large factor. This indicates that at low oxygen concentrations much of the metal escaped from the flame unburned.

For compositions with low metal content, propagation is very difficult. It is believed that the decomposition of excess sodium nitrate removes heat from the burning surface. This heat loss may reduce the rate of vaporization of the metal, causing this vaporization to become the rate controlling step. At the point at which the vaporization rate becomes considerably lower than the rate of oxidation of the metal, the flame will be quenched due to lack of fuel.

CONTENTS

TABLES

FIGURES

INTRODUCTION

The combustion of aluminum-sodium nitrate (Al-NaNO$_3$) flare compositions appears to consist of a two-stage process. In the first process occurring in the flare per se, the oxidizer and/or its decomposition products react with the solid, liquid, or gaseous metal. The second stage, occurring solely in the vapor phase outside the solid flare, consists of the combustion of hot or incandescent metal particles and/or metal vapor, both with gases produced by the oxidizer and with oxygen (O$_2$) from the air.

The object of this study was to investigate the second stage process, primarily that involving the reaction of atmospheric gases with metal particles or vapor. To our knowledge, this type of investigation has not been conducted before; however, it is believed that the extensive investigations of single particle combustion in gases of controlled temperatures and compositions (refs 1,2,3) are directly related to these studies. It was found in previous work by this Laboratory (ref 4) that powdered aluminum (Al), when mixed with various additives, would react vigorously with oxidizing gases well below its melting point, and that the additives which produced these gases from sodium nitrate (NaNO$_3$) at low temperature would cause a large increase in the luminosity when the composition was burned. These results also indicated that experiments should be conducted in which metal-oxidant compositions were burned in atmospheres containing differing amounts of O$_2$ with various diluents such as nitrogen (N$_2$), argon (Ar), or helium (He). This report presents the results obtained in an investigation conducted by this Laboratory into the effect of atmospheric composition on the performance characteristics of burning Al-NaNO$_3$ pyrotechnic compositions.

EXPERIMENTAL PROCEDURE

Samples consisted of 300 to 400 mg of the flare composition capped with 100 to 200 mg of nonilluminating igniter composition. Consolidation was accomplished by pressing the above samples in a 6 mm die at pressures of either 10,000 or 33,000 psi. The pressed pellets formed were about 6 mm long. The pellets were then wrapped with two layers of Kraft paper tape to form a case which prevented side burning.

The combustion chamber was an upright cylindrical chamber 25 cm in diameter by 23 cm in height, with a total volume of 11.5 liters. There was a removable quartz window in the center of the wall for observing the burning pellet. The pellet was placed on a stand in the center of the chamber; the chamber was then filled with the proper gas mixture to a total pressure of 760 torr. The pellet was ignited by a hot wire, and the light intensity produced by the burning was measured by a calibrated RCA 926 Vacuum Phototube (having corrective filters to give response essentially equivalent to that of the human eye) located in front of the window 85 cm from the flame. The voltage developed by the phototube current flowing through a standard resistor was recorded by a fast response oscillograph. The duration of burning was reported in seconds; the burning rate (BR) in cm/min and in./min; the average luminous output (LO) in candles/in^2 of flare surface area; the luminous efficiency (LE) in candle-sec/g of composition; and the adjusted LE in candle-sec/g of Al.

1

At least six pellets were burned in each atmosphere. If the results for a pellet were very far from the average in at least 2 of the 3 reported parameters, the values were discarded and several more pellets were burned. The average deviation for each average value was ± 10 to 15%, and all points were within a standard deviation of 1.96.

Determinations of the amount of Al actually burned in Al-NaNO$_3$ flares were made on the residues from pellets burned in a bomb calorimeter. All of the combustion products were washed with water to remove water-soluble components, then filtered, dried, and weighed. These water-insoluble residues were treated with concentrated NaOH to dissolve the Al (which was the only product soluble in NaOH); the remaining material was then filtered, dried, and weighed again for each sample. Any weight lost from the water-insoluble samples was due to Al which had not reacted; from this the amount of Al consumed by each of the burning flares was determined. This is reported as percent (within ± 5%).

MATERIALS USED

Aluminium powder, atomized, average particle size 6 μ, Alcan Company.

Sodium nitrate powder, average particle size 22 μ, Davies Nitrate Company.

Sodium hydroxide electrolytic pellets, certified ACS grade, Fisher Scientific Company.

Nitrogen gas, 99.9% purity, Linde Corporation.

Oxygen gas, 99.6% purity, Linde Corporation.

Argon gas, 99.995% purity, Linde Corporation.

Helium gas, 99.995% purity, U.S. Government.

RESULTS AND DISCUSSION

Compositions of Al-NaNO$_3$ pressed at 10,000 psi and mixed in proportions of 50-50, 45-55, 40-60, and 35-65 weight percentages and were burned in N$_2$-O$_2$ atmospheres in which the O$_2$ content was 0, 20, 40, 60, 80, and 100 volume percent. The 50% Al composition was also burned in atmospheres containing Ar or He instead of N$_2$. The effect of loading pressure was investigated by studying the 50% Al composition pressed at 33,000 psi and burned in the N$_2$-O$_2$ atmospheres listed above.

2

Effect of Aluminum Content on the Performance Characteristics

Figure 1 (the data plotted in the figures are given in tables 3 through 10) shows that in air the BR's of the compositions pressed at 10 K psi increased sharply with increasing Al content. This effect is attributable to increasing energy feedback from the burning surface to the composition, due to increasing thermal conductivity of the composition. Table 1 shows that the BR's of these systems remained unchanged as the O_2 content was changed, indicating the lack of radiation feedback from the flame zone to the burning surface. In regard to the light output of the compositions, the LO and LE increased as the O_2 content of the atmosphere was increased as shown in figures 2 and 3. The output and efficiency values for the 40 and 45% Al compositions reached plateaus at about 80% O_2 and did not increase as more O_2 was added, while those for the 50% Al composition continued to increase. One would expect a leveling off for compositions containing smaller amounts of Al, for with increasing O_2 concentrations in the atmosphere the compositions cannot supply sufficient metal to the flame zone to effect increasing LO's. However, in this series of experiments the metal deficient 35% Al composition did not plateau as expected.

Table 1. Burning rate of 50-50 aluminum-sodium nitrate in N_2-O_2, He-O_2, and Ar-O_2 atmospheres

% O_2	Burning Rate					
	N_2		He		Ar	
	cm/min	in./min	cm/min	in./min	cm/min	in./min
0	18.4	7.25	17.7	6.97	19.9	7.83
20	19.1	7.51	18.6	7.34	16.9	6.66
40	18.2	7.18	18.0	7.08	16.0	6.32
60	17.1	6.74	18.5	7.28	17.0	6.69
80	18.0	7.10	18.5	7.28	16.0	6.31
100	17.9	7.06	17.9	7.06	17.9	7.06

An interesting effect was noted for low Al compositions. For an Al content of 34% the pellet burned completely in N_2, but propagation became increasingly difficult as the O_2 content of the atmosphere increased, with failure to ignite in pure O_2. The same phenomenon also occurred using compositions containing 32 and 33% Al. This detrimental effect of O_2 on the combustion of low Al content compositions was corroborated by bomb calorimetry studies by others in which difficulty was encountered burning Al in pure O_2 (ref 5).

3

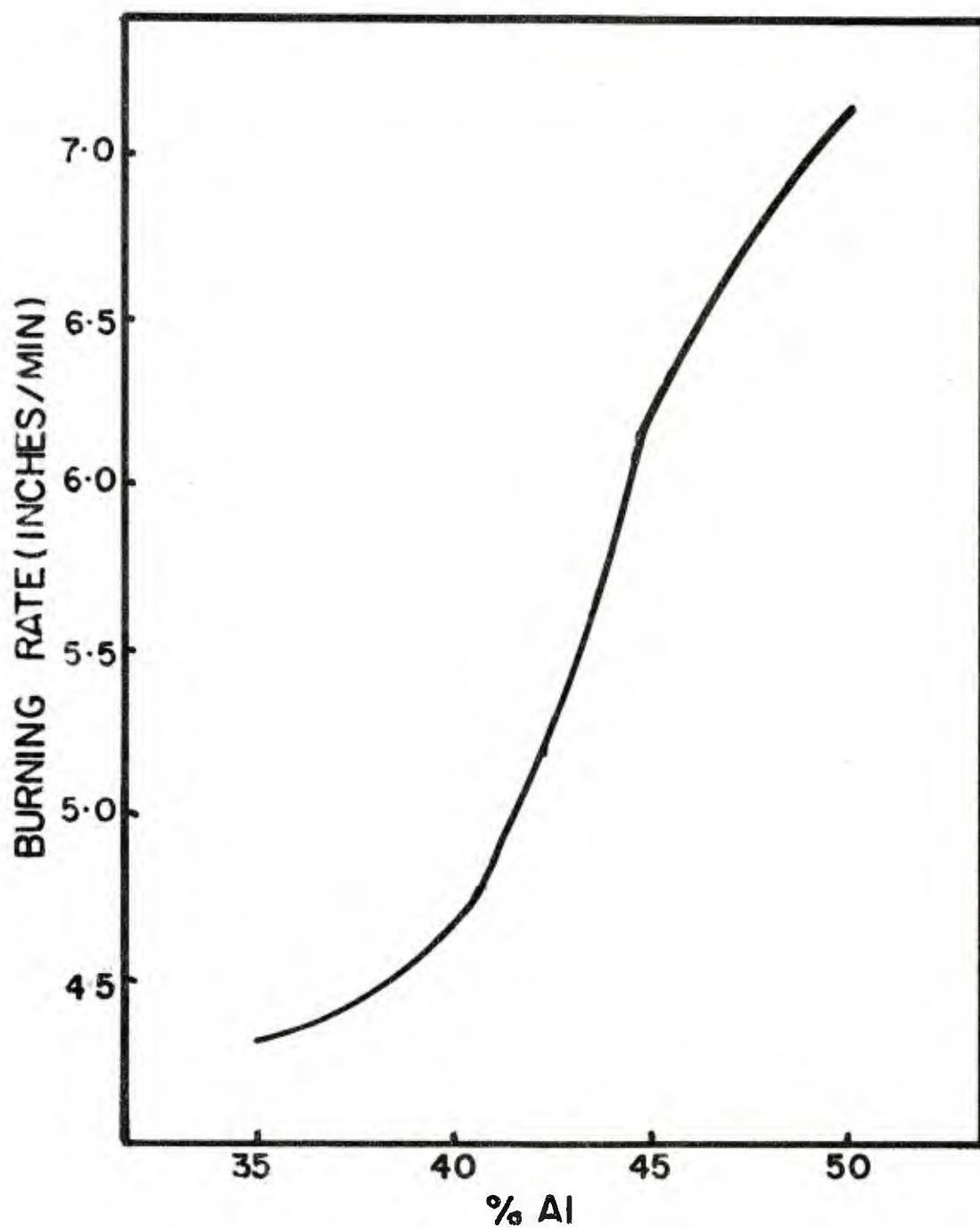Figure 1. Effect of Al content on burning rate of Al–NaNO$_3$ compositions burning in 80% N$_2$ – 20% O$_2$ atmosphere (loading pressure = 10,000 psi)
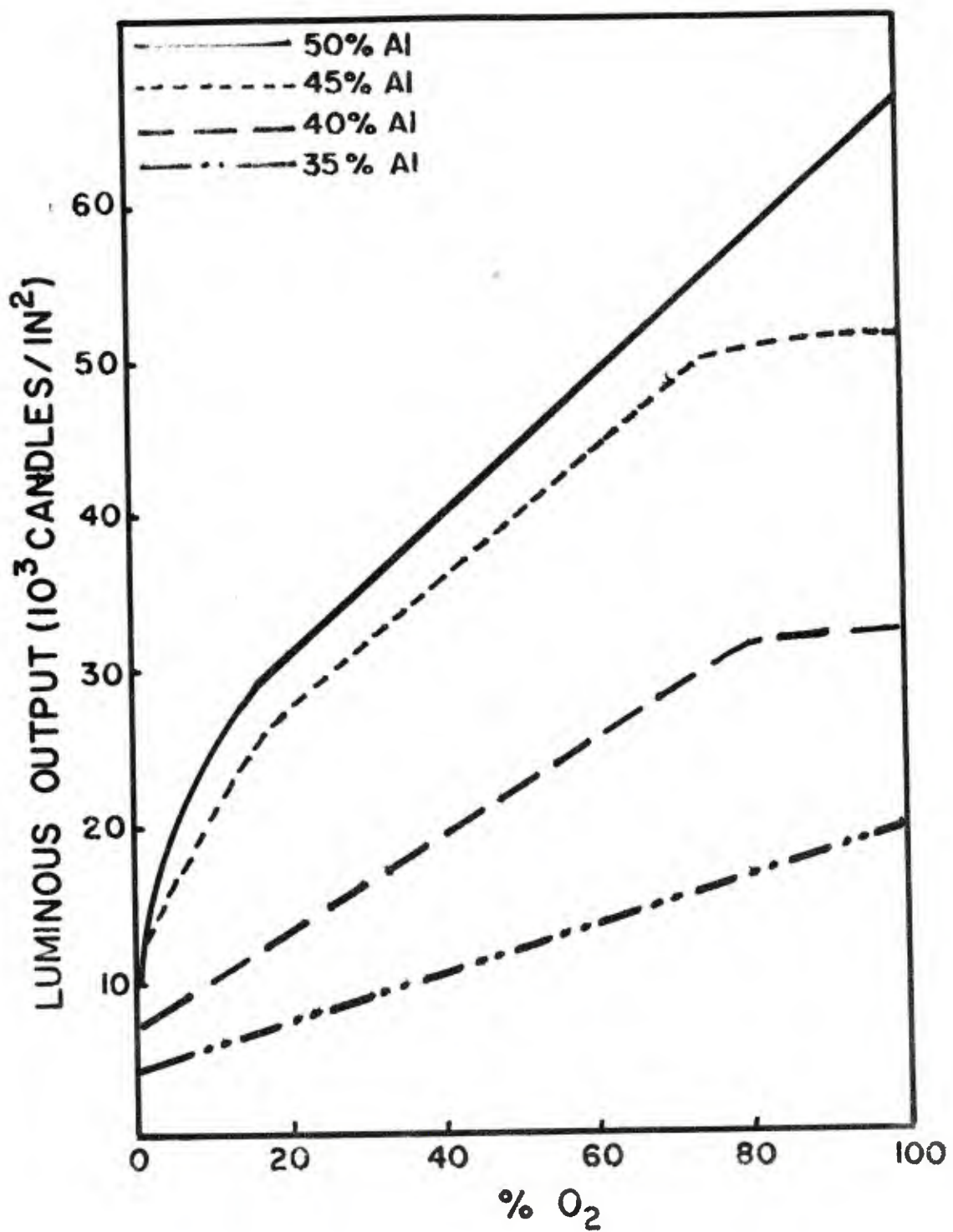
Figure 2. Effect of Al content and atmospheric N_2/O_2 content on luminous output (loading pressure = 10,000 psi)
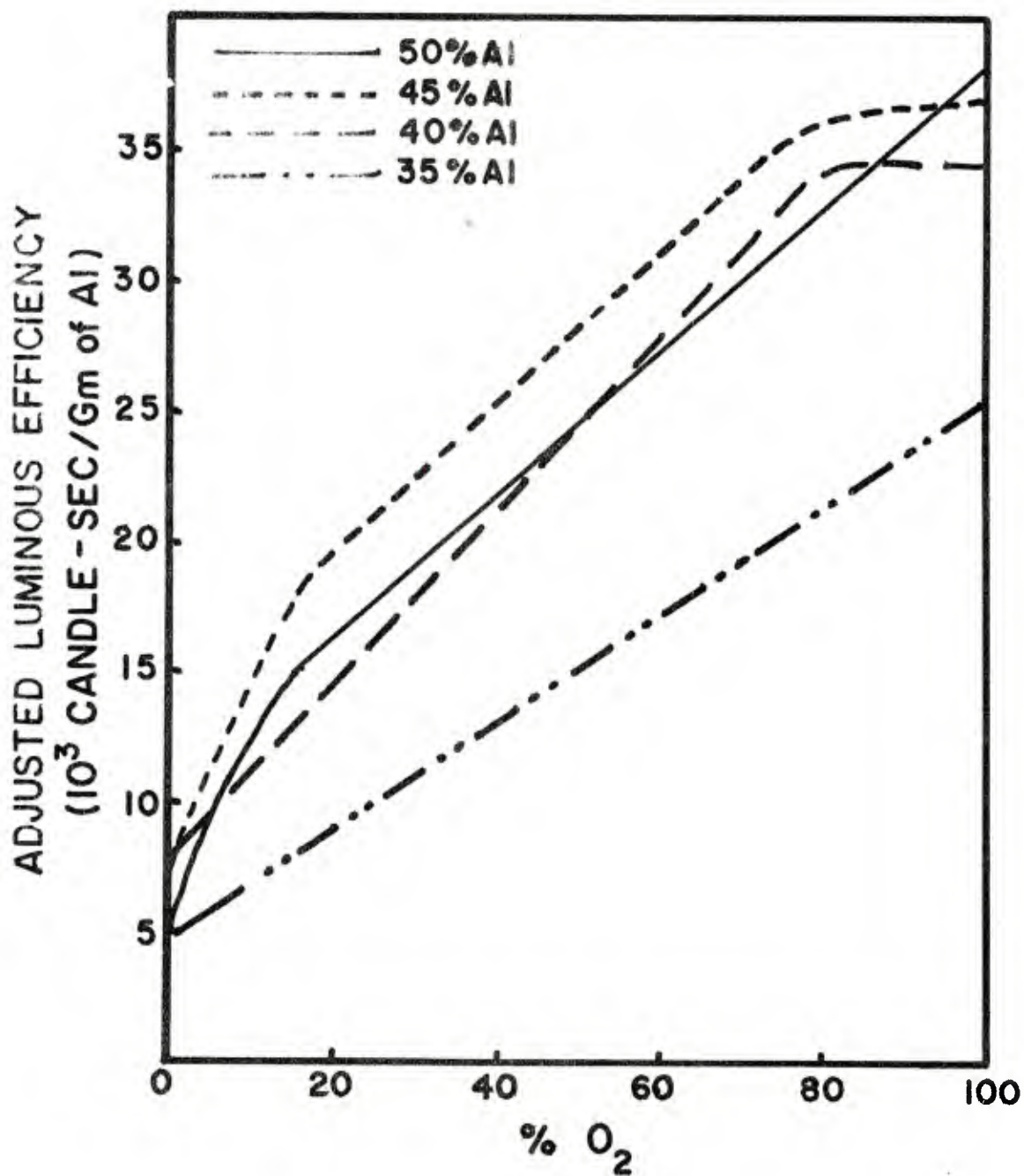
Figure 3. Effect of Al content and atmospheric N_2/O_2 content on adjusted luminous efficiency (based on grams of Al) (loading pressure = 10,000 psi)

The figures also illustrate that with 45 and 50% Al, the LO and LE rose rapidly from 0 to 20% O_2, but the rise became less steep beyond this point, while both parameters increased linearly in this region for 35 and 40% Al.

In order to understand these results, one must examine the spectra produced by these systems. Beardell (ref 6), as well as others working in the field, point out that the radiation produced by pyrotechnic metal/$NaNO_3$ systems is a combination of greybody continuum (white light) produced by hot metal oxide particles, and of broadened sodium D-line emission. Consequently, as the oxide concentration and/or temperature increases, the greybody radiation increases and the flame color changes from yellowish (sodium emission) to whitish. This change in color corresponds to the changes in spectral distributions illustrated in figure 4.

In the present studies, the Al did not burn in the atmosphere when the atmosphere consisted of pure N_2, as shown by the fact that under these conditions the LO is the same as that obtained for the inert gas Ar (see fig. 5). In the N_2 atmosphere, the reaction is as follows:

$$4Al + 2NaNO_3 \rightarrow 2Al_2O_3 + N_2 + 2Na.$$
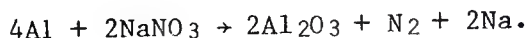
In this reaction, heat is produced, causing sodium D line emission and a small amount of greybody emission from hot metal oxides. In addition, some free Al vapor is also formed which does not burn in the atmosphere. When the O_2 content of the atmosphere is increased, some of the vaporized Al reacts by the equation

$$4Al + 3 O_2 \rightarrow 2Al_2O_3$$
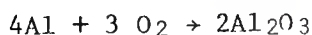
to produce more greybody emission, making the flame whiter in color. The large increase in LO from 0 to 20% O_2 atmosphere for 45 and 50% Al compositions as opposed to 35 and 40% Al is due to the larger amount of Al available to be vaporized and subsequently burned.

Figure 2 shows that the slopes of the various curves increase as the Al content increases. Since the change in slope going from 45 to 50% Al is small, the slope is apparently reaching a constant value. In general, as the compositions become increasingly metal rich, the excess metal begins to act as a strong heat-sink, causing a reduction in the reaction rates of the processes occurring in the condensed phase and leading to eventual reduction in LO.

Table 2 presents the results of analyses conducted to determine the amount of unburned Al present in the combustion products of several of these compositions. It is seen that approximately 90% of the metal in the 40 and 50% Al compositions was consumed when the compositions were burned in pure O_2 atmospheres, but a large amount of Al remained in the residues produced by the 35 and 50% Al compositions burning in 20% O_2 atmospheres.
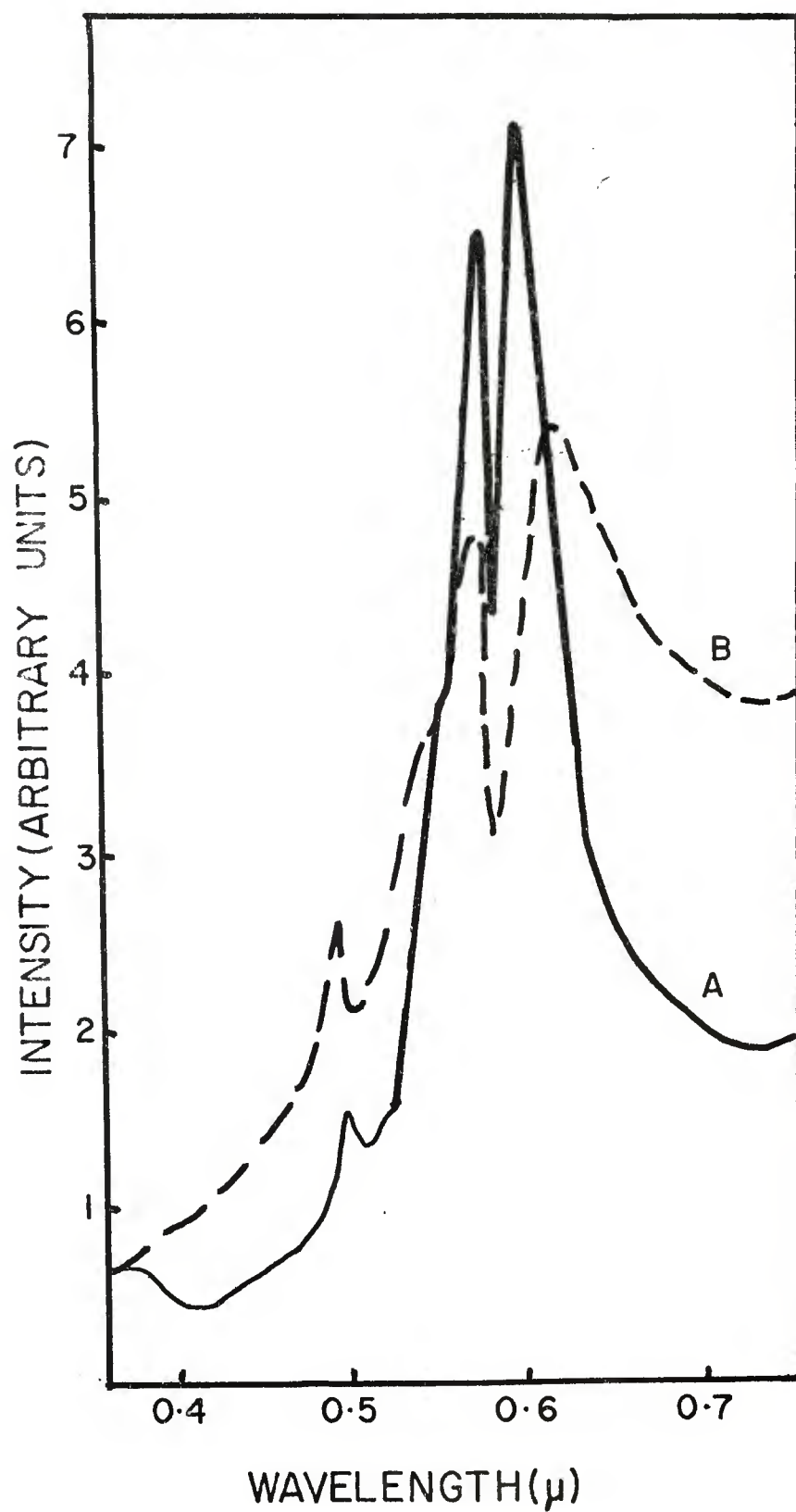
7

Figure 4. Greybody continuum versus resonance line broadened spectra. A. Resonance line broadening predominance. B. Greybody continuum predominance
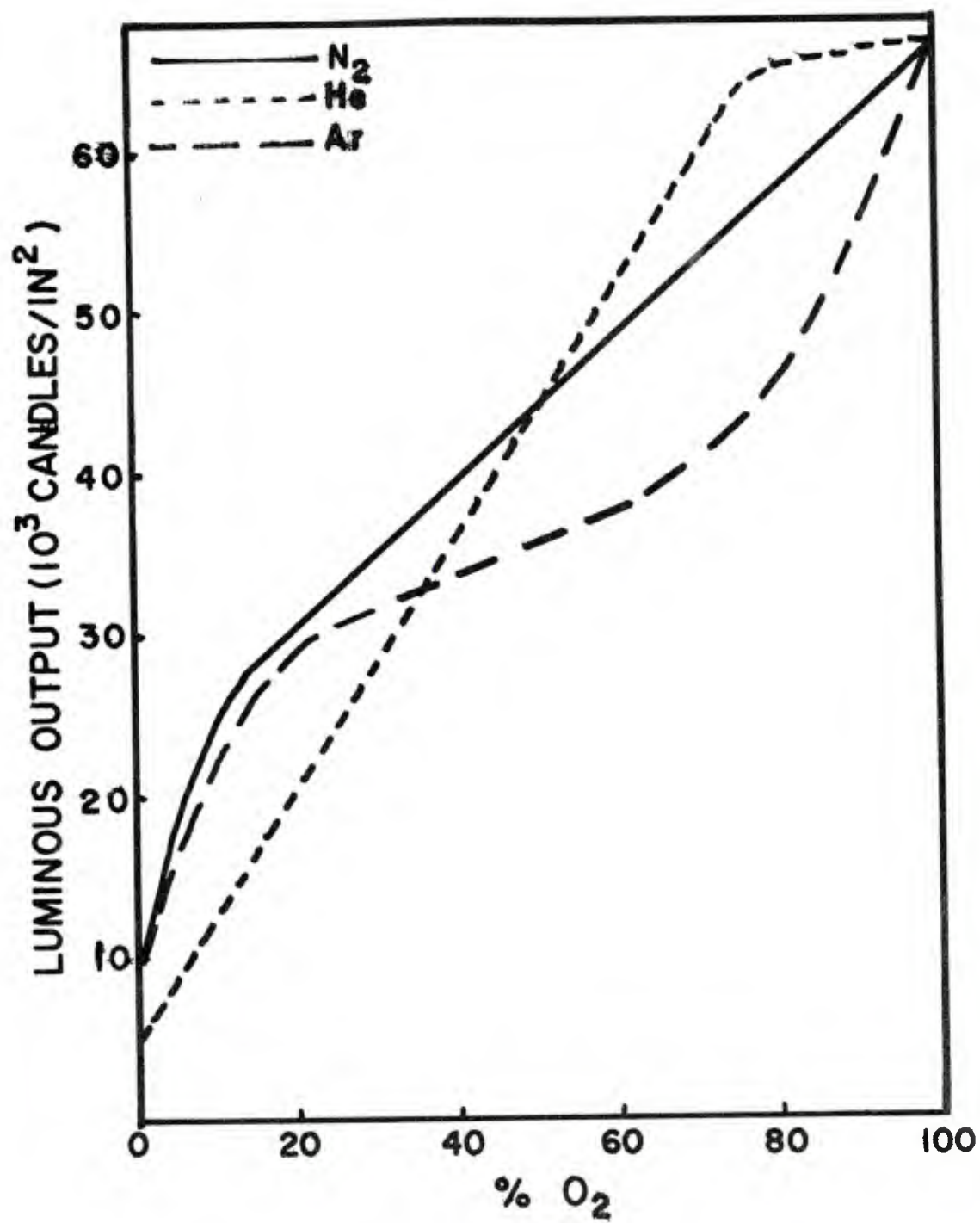
8

Figure 5. Effect of various inert gases on luminous output of 50% Al — 50% NaNO₃ composition (loading pressure = 10,000 psi)

9

Table 2. Amount of aluminum consumed in aluminum-sodium nitrate flares

Composition by weight percentages	% O_2 in atmosphere	Adjusted LE	Normalized adjusted LE	Actual fraction of Al Consumed
A. 50 Al – 50 NaNO$_3$	20	16.9	0.45	0.54
B. 35 Al – 65 NaNO$_3$	20	7.52	0.20	0.30
C. 50 Al – 50 NaNO$_3$	100	37.6	1.00	0.90
D. 40 Al – 60 NaNO$_3$	100	34.5	0.92	0.91

The above data indicate that there may be a correlation between the amount of Al consumed and the light produced by the burning flare. The LE data in figure 3 are based on the light produced per unit weight of Al, rather than on unit weight of composition. This method of representing the data makes it possible to compare directly the relative efficiencies of flares of varying Al compositions. Since the 50% Al composition burning in 100% O_2 produces the highest LE observed in this study, this LE was used as a standard. On this basis, the ratio of the adjusted LE for a given composition to that of the 50% Al-NaNO$_2$ composition burned in 100% O_2 should be a rough measure of the amount of Al consumed. When the ratios were computed and listed in table 2, such a correlation was found. For example, this ratio was 0.45 for a 50% Al composition burned in 20% O_2 whereas the amount of Al actually consumed was 54%; for a 40% Al composition burned in 100% O_2, the ratio was 0.92 while the amount of Al consumed was 91%.

Effect of Inert Gases on the Performance Characteristics

Factors which may also influence the performance of the Al flare are the possibility of reaction with N_2 in the high temperature flame, and heat loss from the flame zone by transfer to the surrounding atmosphere. To study these effects, ambient atmospheres containing He or Ar instead of N_2 were used with compositions containing 50% Al. The O_2 content was again varied between 0 and 100%. The BRs shown in table 1 are essentially constant, irrespective of the inert gas used or its O_2 content. This again indicates that radiative energy feedback to the burning surface is negligible. The substitution of Ar for N_2 had no effect when there was no O_2 in the atmosphere, but had a negative effect on LO at higher O_2 content, as shown in figure 5. This can be explained by less fragmentation of the Al droplets in the flame zone for Ar-O_2 atmosphere. A better understanding of the burning of Al in inert and O_2 bearing atmospheres together with resulting physical processes such as drop fragmentation, can be obtained from the interesting publication on Al and Be burning by Prentice (ref 7). Some important excerpts for the paper are as follows:

1. The stoichiometric oxide formed in the combustion process (Al_2O_3) is insoluble in the metal and nonvolatile at temperatures occurring at the surface of the burning droplet.

2. Oxide accumulation on surface of droplet causes droplet dissymmetry resulting in spinning, oxide shedding, and fragmentation.

3. The behavior of Al burning in O_2/Ar mixtures represents the simplest straightforward burning of Al with no product accumulation on the surface during burning. Burning in this case is a linear function of droplet diameter.

4. Experiments show that N_2, rather than being inert as had been supposed for some time, is an active participant in the combustion of Al in air. Nitrogen appears to be the responsible agent in causing the product to adhere to the droplet surface leading to geometric dissymmetry.

5. Al droplets do not fragment in O_2/Ar.

6. In summarizing the combustion of Al droplets in air and 20/80 O_2/Ar all of the following are pertinent: (1) the droplets spin in air but not in O_2/Ar; (2) the droplets jet in air but not in O_2/Ar; (3) the droplets radiate less intensely in air than in O_2/Ar; (4) the droplets fall more rapidly in air than in O_2/Ar; and (5) the total burn time is shorter in air than in O_2/Ar.

One major difference observed with the different inert gases was a 50% decrease in the LO from a pellet burned in pure He compared to that burned in pure N_2 or pure Ar. The thermal conductivity of He is about 10-fold higher than that of N_2 or Ar (ref 8). The increased thermal conductivity decreases the flame temperature by increased transfer of energy to the surrounding gas. This results in reduction of radiation output produced by the oxidation of Al and reduction in grey body radiation.

Effect of Loading Pressure on the Performance Characteristics

The effect of loading pressure was studied by burning the 50% Al composition consolidated at 10 K and 33 K psi. The composition pressed at the lower pressure displayed a minimal change of BR of 17.0 to 19.1 cm/min (6.7 to 7.5 in./min) with increasing O_2 content, but the BR for the composition consolidated at 33 K psi, decreased from 22.6 to 12.2 cm/min (8.9 to 4.8 in./min) as the atmospheric O_2 concentration increased.

Figure 6 compares the LO's produced by the pellets at the two loading pressures. When burned in pure N_2, the composition loaded at the higher pressure produced somewhat higher LO, due mostly to a slightly higher BR. However, the addition of only 20% O_2 caused a large increase in the LO for the composition loaded at 10 K psi, while that for the composition loaded at 33 K psi changed very little. Since the gaseous permeability of the pellet is reduced by half upon increasing the loading pressure from 10 to 33 K psi, the subsurface heating of fuel from hot gases permeating back into the composition is hindered, resulting in expulsion of metal droplets rather than metal vapor into the flame zone for the composition loaded at 33 K psi. Since these droplets do not burn completely before passing from the flame zone, the LO is reduced.
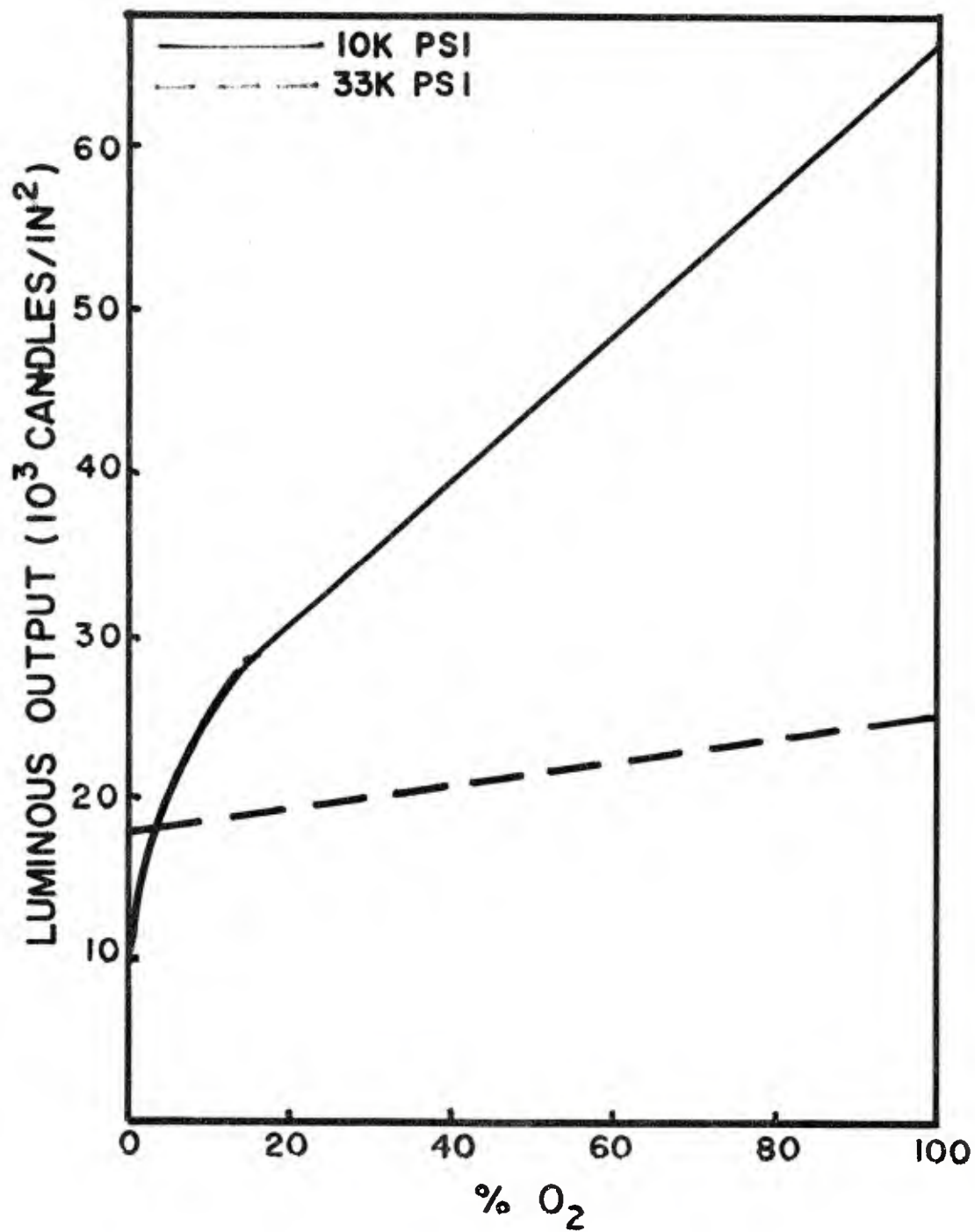
Figure 6. Effect of loading pressure and atmospheric N_2/O_2 content on luminous output of 50% Al - 50% NaNO$_3$ composition

Another problem encountered in the burning of this composition was the loss of fuel from the pellet itself. It was found that when the composition was burned in 20 and 100% O_2 atmospheres, a solidified mass of 20% and 3%, respectively, of the Al in the pellet was left unburned on the stand. This phenomenon did not occur for any other composition or atmosphere.

The cause of this occurrence was the reduction of subsurface heating which allowed the metal to flow from the surface instead of vaporizing; the increase in temperature caused by the addition of O_2 to the atmosphere (ref 9) would help to reduce this problem, and since more of the pellet was burned, would result in apparently longer burning time. However, the expulsion of metal droplets into the flame mentioned above would keep the LO low compared to the composition pressed at 10 K psi.

CONCLUSIONS

The burning process for Al-$NaNO_3$ compositions appears to fall into two parts: one in the condensed phase and the other in the vapor phase. In the condensed phase reaction, the nitrate melts and decomposes, and the Al melts and begins to vaporize. For the compositions pressed at low loading pressure, the above phenomena occur at a rate which is unaffected by the atmospheric composition, evidenced by the constant BR for each composition, and therefore heat and radiation feedback from the flame play a very minor role in the condensed phase process.

The decomposition of excess $NaNO_3$ will remove heat from the compositions with low Al content, resulting in a lower BR and LO (from slower vaporization of Al) and also in a cooler flame. This cooler flame would be very inefficient in burning Al. Indeed, this could cause nonpropagation when, as occurs in high O_2 atmospheres, the burning process proceeds faster than vaporization can supply metal to the flame. The burning process would be slower in N_2, however, and thus propagation would be possible in this atmosphere even for low metal compositions.

Unlike the condensed phase reactions, the vapor phase burning is greatly affected by the atmosphere. Whereas the Al is vaporizing at a steady rate, the fraction of it which is actually burned is determined by the amount of atmospheric O_2, with nearly all being consumed in pure O_2, but with a great deal remaining unburned in 20% O_2. It appears that there are two important processes which govern the combustion of Al. The first is the coalescence of molten metal into large droplets encased in protective oxide shells. These shells inhibit the burning and may enable the droplets to pass through the flame zone unburned. The second factor is fragmentation of the coated droplets followed by complete burning of the fragments. This factor is enhanced by high fractions of both O_2 and Al (ref 10), while the detrimental coalescence is enhanced by high metal content but is affected very little by the atmosphere. We would then have coalescence predominating for all compositions in low O_2 atmospheres, leaving much Al unburned, but with increasing fragmentation to negate this effect as O_2 is increased. Coalescence would be greater for 50% than for 45% Al compositions, and therefore 45% Al produces the highest adjusted efficiency for all compositions studied. Fragmentation falls off more than coalescence as the Al content is reduced so that the composition containing 35% Al, burning in pure O_2, produces an adjusted LE only 70% as great as that for the other compositions, due to its lesser fragmentation.

13

Prentice (ref 7) has shown that there is no fragmenting of Al droplets when burning in $Ar-O_2$ atmospheres, but that there is a great deal of fragmenting when using N_2 instead of Ar. Therefore, in Ar atmospheres, fragmentation which in N_2 atmospheres normally overcomes coalescence in atmospheres with higher O_2 content, is greatly reduced allowing more Al to pass from the flame zone unburned. The effect of this phenomenon can be clearly seen by comparing the LO of compositions burned in N_2 and in Ar containing atmospheres (shown in fig. 5). The LO for the composition burned in $Ar-O_2$ atmospheres drops further and further below that for the composition burned in N_2-O_2 atmospheres as the O_2 content in increased.

When the loading pressure in increased, the condensed phase reactions and vapor phase burning are much more dependent on each other. The vaporization now is strongly affected by the heat from the flame, which is in turn dependent on the amount of O_2 in the atmosphere. This is due to a reduction in the gaseous permeability of the composition, caused by the high loading pressure, which prevents hot gases from permeating back through the composition, to heat Al below the surface. In the hotter flame achieved in high O_2 atmospheres, more of the Al is vaporized and burned, rather than being lost from the pellet. Because more of the pellet is therefore burned, the BR appears to become lower with increasing O_2. However, coalescence is so strongly favored by the close packing of the metal in this composition that much of the Al still escapes from the flame unburned, and consequently the light output remains low.

14

REFERENCES

1. H.C. Christensen, R.H. Knipe, and A.S. Gordon, _Pyrodynamics_, vol 3, 1965, pp 99–119.

2. T.A. Brzustowski and I. Glassman, _Heterogeneous Combustion_, Academic Press, New York, NY, 1965, p 75, p 117.

3. H.M. Cassel and I. Liebman, _Combustion and Flame_, vol 3, 1959, p 467.

4. P.J. Leader, R.P. Westerdahl, and F.R. Taylor, "The Effects of Some Transition Metal Compounds on the Performance Characteristics of Aluminum/Sodium Nitrate Composition, Technical Report 3846, Picatinny Arsenal, Dover, NJ, May 1969.

5. G. Weingarten, (private communication).

6. A.J. Beardell, P.L. Farnell, D. Anderson, and F.R. Taylor, "Analysis of the Potential for the Improvement of Illuminating Flare Performance," WAG-2 Battlefield Illumination Seminars, TTCP, October 1973.

7. J.L. Prentice, _Combustion Science and Technology_, vol 1, 1970, pp 385–398.

8. _Handbook of Chemistry and Physics_, 43rd edition, The Chemical Rubber Co., Cleveland, Ohio, 1965, p E2.

9. N.S. Nelson, D.E. Rosner, L.C. Kurzuis, and H.S. Levin, 12th Symposium (International) on Combustion, The Combustion Institute, Pittsburgh, PA, 1969, p 59.

10. T.A. Brzustowski and I. Glassman, _Heterogeneous Combustion_, Academic Press, New York, NY, 1965, p 41.

Table 3. Effect of aluminum content on burning rate

(Loading pressure = 10,000 psi)

Al % BR	35		40		45		50	
	cm/min	in./min	cm/min	in./min	cm/min	in./min	cm/min	in./min
	10.9	4.29	11.8	4.63	15.8	6.23	18.1	7.14

Table 4. Effect of aluminum content and atmospheric N_2/O_2 content on luminous output

Luminous output (candles per in^2)

$N_2 - O_2$	35% Al	40% Al	45% Al	50% Al
1 - 0	4.25×10^3	7.26×10^3	10.2×10^3	10.2×10^3
0.8 - 0.2	5.33	15.3	28.5	30.5
0.6 - 0.4	10.3	19.1	34.7	40.5
0.4 - 0.6	11.3	23.3	44.1	49.1
0.2 - 0.8	18.0	31.5	51.9	56.1
0 - 1	20.5	33.3	49.8	67.1

Table 5. Effect of aluminum content and atmospheric N_2/O_2 content on luminous efficiency

Luminous efficiency (candles sec/g)

$N_2 - O_2$	35% Al	40% Al	45% Al	50% Al
1 - 0	2.10×10^3	3.00×10^3	3.15×10^3	2.75×10^3
0.8 - 0.2	2.63	6.57	9.08	8.45
0.6 - 0.4	4.84	8.33	10.9	11.2
0.4 - 0.6	5.68	10.3	14.1	14.4
0.2 - 0.8	7.28	13.9	16.8	15.6
0 - 1	8.91	13.8	16.0	18.8

Table 6. Effect of aluminum content and atmospheric N_2/O_2 content on adjusted luminous efficiency (based on g of Al)

Luminous efficiency (candles - sec/g of Al)

$N_2 - O_2$	35% Al	40% Al	45% Al	50% Al
1 - 0	6.01×10^3	7.51×10^3	7.00×10^3	5.58×10^3
0.8 - 0.2	7.52	16.4	20.2	16.9
0.6 - 0.4	13.8	20.8	24.3	22.4
0.4 - 0.6	16.2	25.7	31.3	28.9
0.2 - 0.8	20.8	34.7	37.4	31.3
0 - 1	25.5	34.5	35.5	37.6

18

Table 7. Effect of inert gases on luminous output of 50-50 Al-NaNO$_3$ compositions

Luminous output (candles per in^2)

Gas - O$_2$	N$_2$	He	Ar
1 - 0	10.2×10^3	5.56×10^3	12.4×10^3
0.8 - 0.2	30.5	12.2	30.2
0.6 - 0.4	40.5	35.4	32.6
0.4 - 0.6	49.1	51.9	38.3
0.2 - 0.8	56.1	65.3	45.6
0 - 1	67.1	67.1	67.1

Table 8. Effect of inert gases on luminous efficiency of 50-50 Al-NaNO$_3$ compositions

Luminous efficiency (candles - sec/g)

Gas - O$_2$	N$_2$	He	Ar
1 - 0	2.79×10^3	1.58×10^3	3.16×10^3
0.8 - 0.2	8.45	6.02	8.97
0.6 - 0.4	11.2	9.93	10.2
0.4 - 0.6	14.4	14.1	11.4
0.2 - 0.8	15.6	17.8	14.3
0 - 1	18.8	18.8	18.8

Table 9. Effect of loading pressure and atmospheric N_2/O_2 content on luminous output of 50-50 Al-$NaNO_3$ compositions

Luminous output (candles per in^2)

$N_2 - O_2$	P = 10 K psi	P = 33 K psi
1 - 0	10.2×10^3	17.9×10^3
0.8 - 0.2	30.5	19.4
0.6 - 0.4	40.5	21.6
0.4 - 0.6	49.1	22.1
0.2 - 0.8	56.1	21.9
0 - 1	67.1	25.6

Table 10. Effect of loading pressure and atmospheric N_2/O_2 content on luminous efficiency of 50-50 Al-$NaNO_3$ compositions

Luminous efficiency (candles-sec/g)

$N_2 - O_2$	P = 10 K psi	P = 33 K psi
1 - 0	2.79×10^3	3.36×10^3
0.8 - 0.2	8.45	3.73
0.6 - 0.4	11.2	4.78
0.4 - 0.6	14.4	5.09
0.2 - 0.8	15.6	5.77
0 - 1	18.8	8.88

Commander
U.S. Army Armament Research and
  Development Command
ATTN: DRDAR-GCL
        DRDAR-LCE, Dr. Walker (3)
                   Mr. L. Avrami
                   Mr. L. Frey
                   Mr. G. Jackman
        DRDAR-LCE-T, Mrs. P. Farnell (10)
        DRDAR-LCU, Mr. A.S. Roseff
                   Mr. A. Moss
        DRDAR-SCA
        DRDAR-TSS (5)
Dover, New Jersey 07801

Commander
U.S. Army Armament Materiel
  Readiness Command
ATTN: DRSAR-LEP-L
Rock Island, IL 61299

Commander/Director
Chemical Systems Laboratory
U.S. Army Armament Research and
  Development Command
ATTN: DRDAR-CLJ-L
        DRDAR-CLB-PA
APG, Edgewood Area, MD 21010

Director
U.S. Army Materiel Systems Analysis
  Activity
ATTN: DRXSY-MP
Aberdeen Proving Ground, MD 21005

Director
Ballistics Research Laboratory
U.S. Army Armament Research and
  Development Command
ATTN: DRDAR-TSB-S
Aberdeen Proving Ground, MD 21005

Chief
Benet Weapons Laboratory, LCWSL
U.S. Army Armament Research and
  Development Command
ATTN: DRDAR-LCB-TL
Watervliet, NY 12198

Director
U.S. Army TRADOC Systems
  Analysis Activity
ATTN: ATAA-SL
White Sands Missile Range, NM 88002

Commander
Harry Diamond Laboratories
ATTN: Library, Room 211, Bldg. 92
Connecticut Ave & Van Ness St., N.W.
Washington, DC 20438

U.S. Army Research Office
ATTN: RDRD
P.O. Box 12211
Research Triangle Park, NC 27709

Commander
Naval Weapons Support Center
ATTN: Code 5042, Dr. B. Douda
                 Dr. H. Webster
Crane, IN 47522

Commander
Naval Weapons Center
ATTN: Code 3880, Dr. S. Reed
       Code 233, Technical Library
China Lake, CA 93555

Commander
Naval Surface Weapons Center
White Oak Laboratory
ATTN: Code X-21, Tech Library
Silver Spring, MD 20910

Commander
Naval Air Systems Command
ATTN: Code AIR-310C, Dr. H. Rosenwasser
       Code AIR-954, Technical Library
Washington, DC 20361

Commander
U.S. Naval Ordnance Station
ATTN: Scientific and Tech Info Div
Indian Head, MD 20640

Commander
Naval Sea Systems Command
ATTN: SEA-62R32, Mr. G. Edwards
       SEA-09G3, Technical Library
Washington, DC 20362

Commander
Pacific Missile Test Center
Electro-Optics Division
ATTN: Technical Library
Pt. Mugu, CA 93042

Aeronautical Systems Division (AFSC)
ATTN: Technical Library
Wright-Patterson Air Force Base
Ohio 45433

Commander
U.S. Air Force
ATTN: AFATL/DLOSL
Eglin Air Force Base, FL 32542

Commander
Armament Development Test Center
ATTN: Code ADTC/SDWE
Eglin Air Force Base, FL 32542

Commander
Lowry Technical Training Center (TTOX)
Lowry AFB, CO 80230

Commander
Air Force Avionics Laboratory (AFSC)
ATTN: AFAL/WRW-3, Mr. F.E. Linton
                Mr. R.D. Hunziker
       AFAL-WRD-2, Mr. G.W. Schivley
Wright Patterson Air Force Base, OH 45433

Central Intelligence Agency
ATTN: CRS/ADD/Standard Distribution
Washington, DC 20505

U.S. Army Foreign Science and
   Technology Center
ATTN: DRXST-CSI, Mr. J. Jacoby
220 Seventh St., NE
Charlottesville, VA 22901

Institute for Defense Analyses
ATTN: Library, Documents
400 Army-Navy Drive
Arlington, VA 22201

Administrator
Defense Technical Information Center
ATTN: Accessions Division (12)
Alexandria, VA 22314

Denver Research Institute
University of Denver
Denver, CO   80220

Battelle Memorial Institute
Columbus Laboratories
TACTEC
505 King Avenue
Columbus, OH   43201